Bull. Chem. Soc. Jpn., ***65***, *2505—2509 (1992)*

ESR Study of Active Oxygen Radicals from Photoexcited Semiconductors Using the Spin-Trapping Technique

Hiroyuki NODA,* Kazuo OIKAWA,† and Hitoshi KAMADA
Division of Life Support Technology, Yamagata Technopolis Foundation,
683 Kurumanomae, Numagi, Yamagata 990
† Yamagata Research Institute of Technology,
683 Kurumanomae, Numagi, Yamagata 990
(Received April 27, 1992)

The ESR spin-trapping technique was used to detect active oxygen radicals by photoexcitation of powdery semiconductors (TiO_2, WO_3, CdS, and Fe_2O_3) in water and aqueous H_2O_2 solutions using 5,5-dimethyl-1-pyrroline *N*-oxide (DMPO) as spin trap. Superoxide ion (O_2^-), hydroperoxyl radical ($\cdot O_2H$) and hydroxyl radical ($\cdot OH$) were detected under photoexcitation. The mechanism for the generation of active oxygen radicals is discussed referring to the energy band structures of the semiconductors and the redox potentials of the oxygen radicals.

Powdery semiconductors (TiO_2, CdS, WO_3, Fe_2O_3, etc.) are used for photosynthetic and photocatalytic reactions,[1-5] and many papers have been published on the photocatalysis on powdery TiO_2 exhibiting strong oxidation capability.[6-10] Biological use of TiO_2 has also been attempted: Kamioka et al.[11] used TiO_2 to cleave double-stranded DNA and Cai et al.[12] used it as a cancer killing agent.

The spin-trapping technique, widely used for detection of short-lived radicals,[13] has been used in the past decade to detect spin adducts in the photocatalytic reactions of semiconductor suspensions.[14-18] Superoxide ion was detected by photoexcitation of CdS in aqueous media.[14] Hydroxyl and hydroperoxyl radicals were detected by photoexcitation of anatase TiO_2 in aqueous media using α-phenyl-*N*-*t*-butylnitron (PBN) and 4-pyridylmethyleneamine *N,N'*-dioxide (4-POBN) as spin traps.[15] Hydroxyl radical was also detected with rutile TiO_2 in aqueous media using 5,5-dimethyl-1-pyrroline *N*-oxide (DMPO) as spin trap.[17] However, the mechanism for the generation of active oxygen radicals from photoexcited semiconductors is not yet clear. We have carried out experiments that involve spin-trapping of intermediates produced during irradiation of powdery semiconductors in water and aqueous H_2O_2 solutions, to examine the mechanism of active oxygen radical generation in the photocatalysis.

Experimental

Materials. Powdery semiconductors [TiO_2 (99.9%, rutile and anatase), CdS (practical grade), WO_3 (99.5%), and Fe_2O_3 (99.9%)] were obtained from Wako Pure Chemical Industries, Ltd. 5,5-Dimethyl-1-pyrroline *N*-oxide (DMPO) was purchased from Dojindo Laboratory. Hydrogen peroxide (H_2O_2, 30% aqueous solution, Wako Pure Chemical Industries, Ltd), superoxide dismutase (SOD, Cu/Zn, Sigma) and ethanol (99.5%, Kanto Chemical Co., Inc) were also used in the experiments.

Apparatus. A flat, quartz ESR cell was used in all the experiments. A powdery semiconductor (1—5 mg) was mixed with 100 µl of distilled water (or 0.1 mol dm^{-3} H_2O_2), 20 µl of ethanol (or distilled water) and 30 µl of 0.46 mol dm^{-3} DMPO. The suspension was then fed into the ESR cell, which was inserted into the cavity of an ESR spectrometer (JEOL JES-RE3X). The sample was irradiated with a 500 W xenon lamp for 60 s. A 370-nm or 420-nm interference filter was used for illuminating TiO_2 or other semiconductors, respectively, there by causing bandgap excitation but excluding the effect of short wavelength ultraviolet light. ESR measurements were conducted under the following conditions: magnetic field, 336±5 mT; field modulation, 0.1 mT; time constant, 0.03 or 0.1 s; receiver gain, 100 or 200; microwave power, 8 mW; sweep time, 5 mT min^{-1}.

Results and Discussion

Reaction on Powdery TiO_2. ESR spectra were observed when TiO_2 (anatase or rutile) was irradiated with photons of energy exceeding the bandgap energy (3.2 or 3.0 eV). Therefore, a 370-nm (3.3 eV) interference filter was used in the following experiments.

ESR spectra observed by excitation of the TiO_2 (2 mg, anatase and rutile)/H_2O/DMPO system at room temperature are shown in Fig. 1. The spectrum of Fig. 1A is composed of signals from hydroxyl radical spin adducts in view of the hfsc values of $a_N = a_H{}^{\beta} = 1.49$ mT.[19] The spectrum of Fig. 1C is composed of signals from superoxide ion (weak signal) and hydroxyl radical spin adducts. Jaeger and Bard[15] observed no ESR signal from rutile TiO_2 by use of PBN and 4-POBN. However, PBN spin adducts of hydroxyl radical were observed for rutile TiO_2 in our experiments. The cause for this discrepancy is not clear, but may be related to the particle size and preparation conditions. The signal intensity of hydroxyl radicals from anatase TiO_2 was larger than that from rutile: This is line with a higher photocatalytic activity of the anatase.[20,21] The DMPO spin adducts of superoxide ion were observed for rutile but not for anatase. This result may be related to the activity of the particle surface, and is to be substantiated by experiments under alkaline conditions described later.

Ethanol was added in these systems to confirm the production of free hydroxyl radical. Addition of

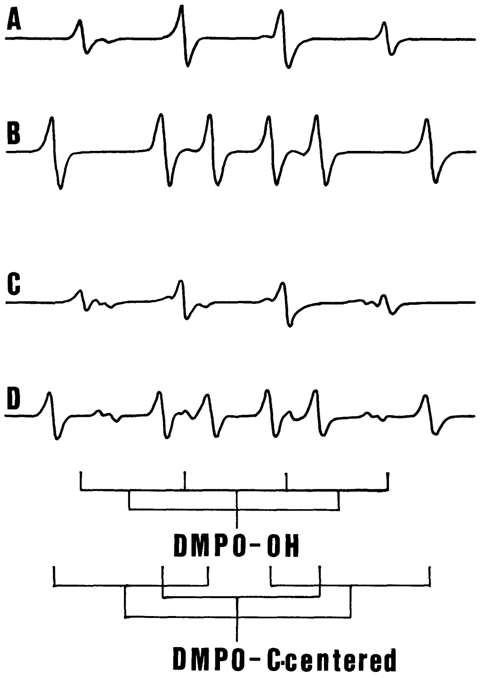

Fig. 1. ESR spectra of DMPO spin adducts obtained by 60-s irradiation of TiO_2 aqueous suspensions. A: anatase, B: A+C_2H_5OH, C: rutile, D: C+C_2H_5OH, receiver gain: ×100, irradiation wavelength: 370 nm.

ethanol quickly converted the hydroxyl radical into a carbon(C)-centered radical as seen in Figs. 1B and 1D. These spectra can be assigned to DMPO spin adducts of C-centered radicals with hfsc values of a_N=1.58 mT and $a_H{}^\beta$=2.28 mT.[19] This evidences the production of free hydroxyl radical and the occurrence of the following reactions.

$$\cdot OH + CH_3CH_2OH \rightarrow \cdot CH(CH_3)OH + H_2O \quad k=1\times10^9\ M^{-1}\,s^{-1\ 22)} \tag{1}$$

$$\cdot CH(CH_3)OH + DMPO \rightarrow DMPO\text{-}CH(CH_3)OH \quad (k\text{: unknown}) \tag{2}$$

The signal intensity of DMPO–C-centered adducts was larger than that of DMPO–OH adducts. These results suggest that reactions (4) and (5) took place, because the rates of reactions (4) and (5) are larger than that of reaction (3).

$$\cdot OH + DMPO \rightarrow DMPO\text{–}OH \quad k=3.4\times10^9\ M^{-1}\,s^{-1\ 19)} \tag{3}$$

$$\cdot OH + O_2^- + H^+ \rightarrow H_2O + O_2 \quad k=1\times10^{10}\ M^{-1}\,s^{-1\ 23)} \tag{4}$$

$$\cdot OH + \cdot OH \rightarrow H_2O \quad k=5\times10^9\ M^{-1}\,s^{-1\ 23)} \tag{5}$$

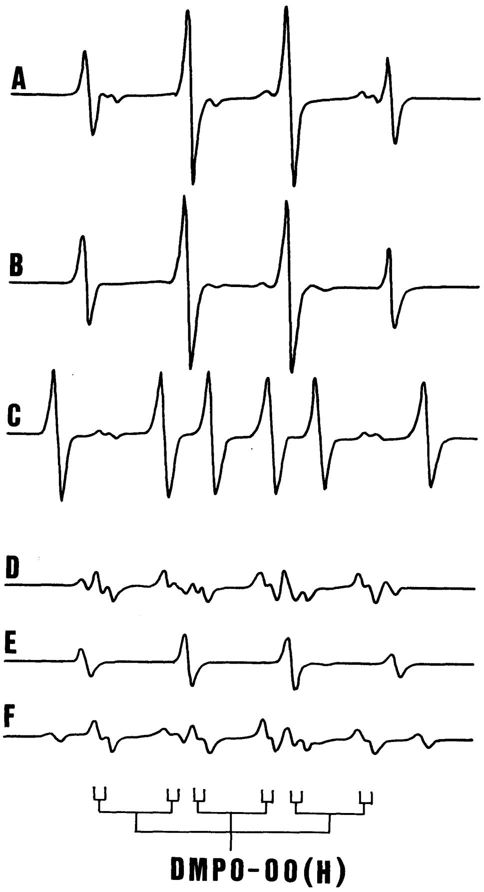

Fig. 2. ESR spectra of DMPO spin adducts obtained by 60-s irradiation of TiO_2 aqueous suspensions containing 0.01 mol dm^{-3} NaOH. A: anatase, B: A+SOD, C: A+C_2H_5OH, D: rutile, E: D+SOD, F: D+C_2H_5OH, receiver gain: ×100(C), ×200 (others), irradiation wavelength: 370 nm.

ESR spectra from the TiO_2 (2 mg)/0.01 mol dm^{-3} NaOH/DMPO system are shown in Fig. 2. The alkaline conditions were used to lengthen the lifetime of superoxide ion in comparison with that in distilled water.[23] The spectra of Figs. 2A and 2D are composed of signals from the hydroxyl radical and superoxide ion spin adducts. The DMPO spin adducts of superoxide ion can be so assigned with hfsc values of a_N=1.41 mT, $a_H{}^\beta$=1.13 mT, and $a_H{}^\gamma$=0.13 mT.[14] The spin adducts of superoxide ion disappeared on addition of superoxide dismutase (SOD, 300 units cm^{-3}) as shown in Figs. 2B and 2E. This evidences the generation of superoxide ion from dissolved oxygen in the TiO_2 suspensions. Under alkaline conditions, the spin adducts of superoxide ion were detected with anatase TiO_2 due to its longer lifetime than in distilled water. The difference between rutile and anatase may have arisen from the surface acidity. The pH of an anatase suspension was lower than that of a rutile suspension under these conditions. The semiconductor surface acidity may hence control the lifetime of superoxide ion. Furthermore, the crystal structure influenced the production of hydroxyl radicals under alkaline conditions. This difference is not clear, but may be also related to the surface acidity which is caused by the dissociation of surface OH bond.[24] The spin adduct of a C-centered radical was also observed on addition of ethanol. Under acidic conditions, the ESR signal intensity with rutile and anatase was slightly lower than those in Fig. 1. This suggests that the presence of proton promoted reaction (4).

ESR spectra for the $TiO_2/0.077\ mol\ dm^{-3}\ H_2O_2/$DMPO system are shown in Fig. 3. The observed spin adducts are for hydroxyl and hydroperoxyl radicals, irrespective of the crystal structure.

The energy band structure of anatase TiO_2 in illustrated in Fig. 4. Photoexcitation of TiO_2 creates electron-hole pairs in the lattice. The potential for reduction of oxygen to superoxide ion lies below the conduction band edge of TiO_2, and the potential for oxidation of H_2O to hydroxyl radical lies above the valence band edge. A photogenerated electron-hole pair is thus sufficiently energetic to produce superoxide ion and hydroxyl radical from H_2O. In the presence of H_2O_2, the potential for reduction of H_2O_2 to hydroxyl radical lies below the conduction band edge of TiO_2, and the potential for oxidation of H_2O_2 to the hydroperoxyl radical lies above the valence band edge. Therefore, hydroxyl and hydroperoxyl radicals can be easily generated in the presence of H_2O_2. To substantiate this, an experiment was carried out on the relation between the concentration of H_2O_2 and the production of active oxygen radicals. An increase in the H_2O_2 concentration indeed led to an increase in the spin adducts of hydroperoxyl radical. And an increase in the H_2O_2 concentration up to 1 mmol dm^{-3} led to an increase in the spin adducts of hydroxyl radical, but an increase in the H_2O_2 concentration over 1 mmol dm^{-3} led to no increase in the spin adducts of hydroxyl radical. That the hydroxyl radical is produced exclusively from the reduction of H_2O_2 has been verified by use of ^{17}O-labeled water at this concentration. Therefore, hydroxyl radical is produced from the reduction of H_2O_2 by photogenerated electrons, and hydroperoxyl radical is produced from the oxidation of H_2O_2 by photogenerated holes under these conditions.

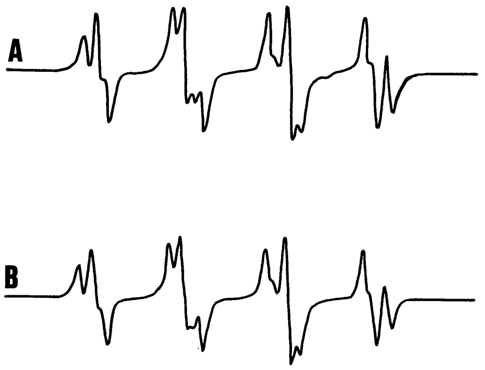

Fig. 3. ESR spectra of DMPO spin adducts obtained by 60-s irradiation of TiO_2 aqueous suspensions containing 0.1 mol dm^{-3} H_2O_2. A: anatase, B: rutile, receiver gain: ×200, irradiation wavelength: 370 nm.

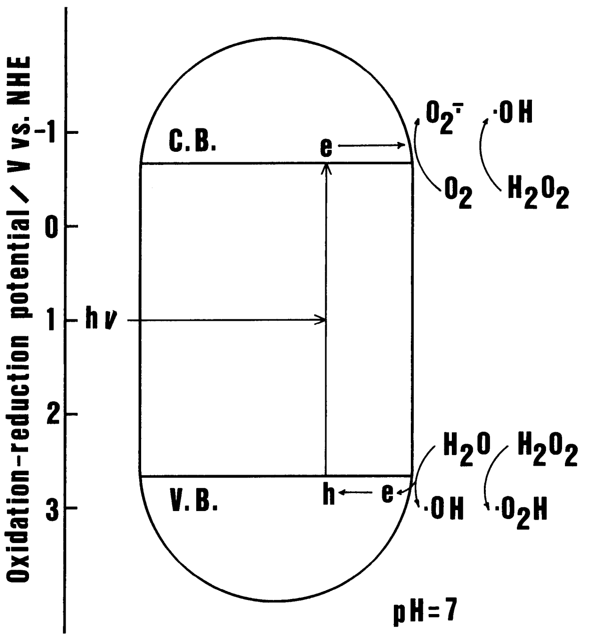

Fig. 4. Energy band structures of TiO_2 (anatase) and the mechanism for the generation of active oxygen radicals in water and aqueous H_2O_2 solutions.

Reaction on Other Semiconductors. The mechanism for the generation of active oxygen radicals would be clarified by experiments with various semiconductors having different energy band structures. ESR spectra were observed when powdery CdS, WO_3, and Fe_2O_3 were irradiated with photons of energy greater than the bandgap energy (2.4, 2.8, and 2.2 eV, respectively). The use of a 420-nm (3.0 eV) interference filter therefore ensures bandgap excitation for three semiconductors. ESR spectra from CdS, WO_3, and Fe_2O_3 aqueous suspensions are depicted in Fig. 5. The DMPO spin adduct of superoxide ion was observed in the CdS suspension, in line with the results of Harbour and

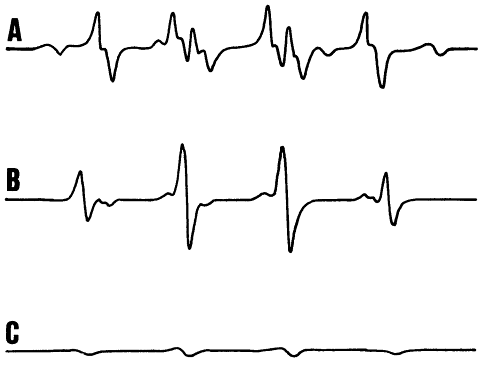

Fig. 5. ESR spectra of DMPO spin adducts obtained by 60-s irradiation of aqueous suspensions of powdery semiconductors. A: CdS, B: WO_3, C: Fe_2O_3, receiver gain: ×100 (B), ×200 (others), irradiation wavelength: 420 nm.

Hair.[14] The six line weak ESR signal come from dimethyl surfoxide, which was added to avoid the influence of sulfide radicals produced by the action of photogenerated holes. No DMPO spin adduct of superoxide ion was detectable after addition of SOD. These results suggest that the potential for reduction of oxygen to superoxide ion lies below the conduction band edge of CdS, but the valence band edge is above the potential for oxidation of H_2O to hydroxyl radical. Photogenerated holes are consumed for the decomposition of CdS.

The DMPO spin adducts of superoxide ion and hydroxyl radical were observed in WO_3 suspension. This is because the potential for reduction of oxygen to superoxide ion is close to the conduction band edge of WO_3, and the potential for oxidation of H_2O to hydroxyl radical is above the valence band edge. Addition of ethanol changed quickly the hydroxyl radical to a C-centered radical.

In Fe_2O_3 suspensions, a very weak ESR signal was observed. This signal did not increased by irradiation, and is hence regarded as the background. Therefore, electron-hole pairs photogenerated in Fe_2O_3 is not energetic enough to produce active oxygen radicals in water. No change in the signal intensity of DMPO spin adducts was noted for CdS, WO_3, and Fe_2O_3 suspensions in going from pure water to alkaline or acidic aqueous solutions.

ESR spectra from CdS, WO_3, and Fe_2O_3 suspensions in the presence of H_2O_2 are given in Fig. 6. For CdS a weak ESR signal was observed. This signal did not increase by irradiation, and is hence regarded as the background. This may be because the decomposition potential of CdS is close to the potential for reduction of H_2O_2.[25] In WO_3 and Fe_2O_3 suspensions, the DMPO spin adducts of hydroxyl and hydroperoxyl radicals were observed since the redox potentials of active oxygen radicals lie between the valence band and conduction band edges.

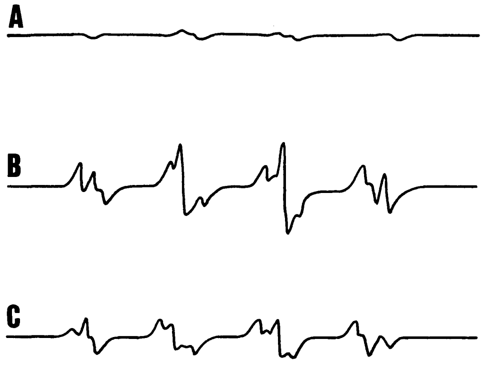

Fig. 6. ESR spectra of DMPO spin adducts obtained by 60-s irradiation of aqueous suspensions of powdery semiconductors in the presence of 0.1 mol dm^{-3} H_2O_2. A: CdS, B: WO_3, C: Fe_2O_3, receiver gain: ×200 (A), ×100 (others), irradiation wavelength: 420 nm.

The energy band structures of semiconductors[26] and redox potentials of active oxygen radicals[14,15] are depicted in Fig. 7. The present results could be rationalized referring to this energy level diagram.

Conclusions

The mechanism for the generation of acitve oxygen radicals from photoexcited semiconductor suspensions has been examined by use of the spin-trapping technique. The results are summarized as follows.

1. In water, superoxide ion is produced from the reduction of dissolved oxygen by photogenerated electrons, and hydroxyl radical is produced from the oxidation of water by photogenerated holes.

2. In the presence of H_2O_2, hydroxyl radical is produced from the reduction of H_2O_2 by photogenerated electrons, and hydroperoxyl radical is produced from the oxidation of H_2O_2 by photogenerated holes, as was

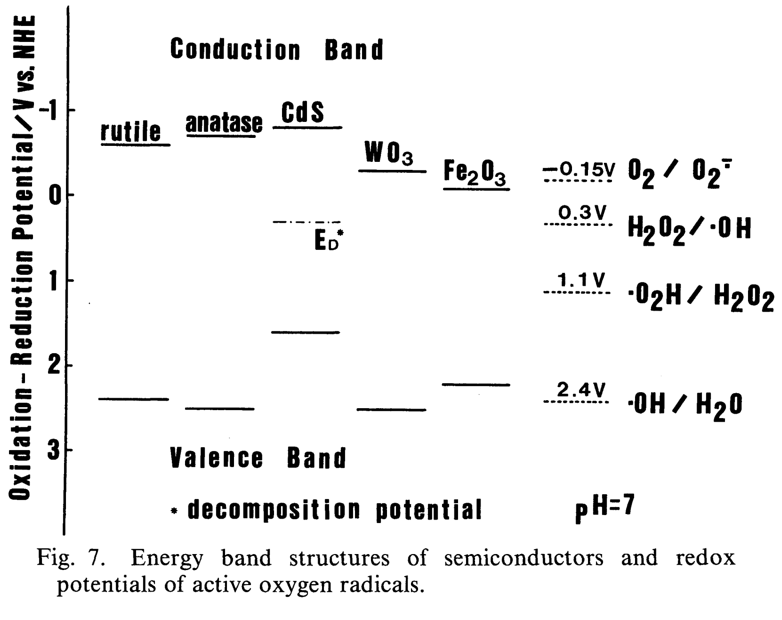

Fig. 7. Energy band structures of semiconductors and redox potentials of active oxygen radicals.

verified by examining the H_2O_2 concentration dependence of ESR signals.

3. The generation of active oxygen radicals from powdery semiconductors in water and aqueous H_2O_2 solutions can be rationalized in terms of the energy band structures of semiconductors and the redox potentials of active oxygen radicals.

The authors wish to express their thanks to Professor Akira Fujishima and Dr. Kazuhito Hashimoto, The University of Tokyo, for thier helpful discussions. This study was performed through Special Coordination Funds of the Science and Technology Agency and the Yamagata Technopolis Foundation.

References

1) M. Grätzel, *Ber. Bunsen-Ges. Phys. Chem.*, **84**, 981 (1980).

2) T. Kawai and T. Sakata, *Nature,* **286**, 474 (1980).

3) K. Kalyanasudaram, E. Borgarello, and M. Grätzel, *Helv. Chim. Acta,* **64**, 362 (1981).

4) B. Anrian-Blajeni, M. Halmann, and J. Manasen, *Sol. Energy,* **25**, 165 (1980).

5) G. N. Schrauzer and T. D. Guth, *J. Am. Chem. Soc.*, **99**, 7189 (1977).

6) S. Sato and J. M. While, *Chem. Phys. Lett.*, **70**, 131 (1980).

7) T. Kanno, T. Oguchi, H. Sakuragi, and K. Tokumaru, *Tetrahedron Lett.*, **21**, 467 (1980).

8) I. Izumi, W. W. Dunn, K. O. Wilbourn, F. -R. F. Fan, and A. J. Bard, *J. Phys. Chem.*, **84**, 3207 (1980).

9) H. Reiche and A. J. Bard, *J. Am. Chem. Soc.*, **101**, 3127 (1979).

10) K. Hashimoto, T. Kawai, and T. Sakata, *J. Phys. Chem.*, **88**, 4083 (1984).

11) H. Kamioka, M. Suzuki, E.Tamiya, and I. Karube, *J. Mol. Catal.*, **54**, 1 (1989).

12) R. Cai, K. Hashimoto, K. Itoh, Y. Kubota, and A. Fujishima, *Bull. Chem. Soc. Jpn.*, **64**, 1268 (1991).

13) E. G. Janzen, *Acc. Chem. Res.*, **4**, 31 (1971).

14) J. R.Harbour and M. L. Hair, *J. Phys. Chem.*, **81**, 1791 (1977).

15) C. D. Jaeger and A. J. Bard, *J. Phys. Chem.*, **83**, 3146 (1979).

16) E. M. Cresa, L. Burlamacchi, and M. Visca, *J. Mater. Sci.*, **18**, 289 (1983).

17) J. R. Harbour and M. L. Hair, *Adv. Colloid Interface Sci.*, **24**, 103 (1986).

18) A. Maldotti, R. Amadelli, and V. Carassiti, *Can. J. Chem.*, **66**, 76 (1988).

19) E. Finkelstein, G. M. Rosen, and E. J. Ranckman, *J. Am. Chem. Soc.*, **102**, 4994 (1980).

20) S. Nishimoto, B. Ohtani, A. Sakamoto, and T. Kagiya, *Nippon Kagaku Kaishi,* **1984**, 246.

21) H. Noda, K. Oikawa, T. Ogata, K. Matsuki, and H. Kamada, *Nippon Kagaku Kaishi,* **1986**, 1084.

22) R. A. Greenwald, "Handbook of Method for Oxygen Radical Research," CRC Press, Florida (1985), p. 151.

23) Nippon Kagaku Kai, Kikan Kagaku Sosetsu No. 7, "Kassei Sanso No Kagaku," Gakkai Shuppan Center, Tokyo (1990), p. 3.

24) K. Kobayakawa, Y. Nakazawa, M. Ikeda, Y. Sato, and A. Fujishima, *Ber. Bunsen-Ges. Phys. Chem.*, **94**, 1438 (1990).

25) T. Inoue, T. Watanabe, A. Fujishima, and K. Honda, *Bull. Chem. Soc. Jpn.*, **52**, 1243 (1979).

26) Nippon Kagaku Kai, "Kagaku Sosetsu No. 39, Muki Kokagaku," Gakkai Shuppan Center, Tokyo (1983), p. 118.